© Indian Academy of Sciences

Review

Relativistic Disc Line: A Tool to Constrain Neutron Star Equation of State Models

SUDIP BHATTACHARYYA

Department of Astronomy and Astrophysics, Tata Institute of Fundamental Research, 1 Homi Bhabha Road, Mumbai 400 005, India.
E-mail: sudip@tifr.res.in

Abstract. Relativistic iron Kα spectral emission line from the inner disc of a neutron star Low-Mass X-ray Binary (LMXB) was first detected in 2007. This discovery opened up new ways to probe strong gravity and dense matter. The past decade has seen detections of such a line from many neutron star LMXBs, and confirmation of this line from the same source with several X-ray satellites. These have firmly established the new field of relativistic disc line from neutron star systems in only a decade or so. Fitting the shape of such a line with an appropriate general relativistic model provides the accretion disc inner edge radius to the stellar mass ratio. In this review, we briefly discuss how an accurate measurement of this ratio with a future larger area X-ray instrument can be used to constrain neutron star equation of state models.

Keywords. Accretion—accretion discs—equation of state—methods: numerical—stars: neutron—X-rays: binaries

1. Introduction

Knowledge of the cold degenerate matter (e.g., $\sim 10^8$ K) at several times nuclear saturation density is a fundamental goal of physics. Such high-density matter may be in exotic states such as pion or kaon condensates, or strange quark matter. Such matter cannot be studied with observations of the early Universe or by heavy-nuclei collision experiments (Blaschke *et al.* 2008; Lattimer & Prakash 2007; Özel & Psaltis 2009; van Kerkwijk 2004). However, this super-dense degenerate matter exists in the cores of neutron stars, and plausibly the only way to probe it is by ruling out as many theoretically proposed Equation of State (EoS) models of the stellar core as possible.

But how to constrain EoS models of the deep interior of a neutron star? While the internal constitution of a neutron star depends on the EoS model, which connects the total mass-energy density (ϵ) with the pressure (p) in a degenerate condition, such a model also determines the stellar bulk properties. For example, the stellar global structure can be computed from the Tolman–Oppenheimer–Volkoff (TOV) equation:

$$\frac{\mathrm{d}p(r)}{\mathrm{d}r} = -\frac{G}{c^2}\frac{[p(r)+\epsilon(r)][m(r)+4\pi r^3 p(r)/c^2]}{r(r-2Gm(r)/c^2)},$$

(1)

if the star is non-spinning. Here, $m(r) = 4\pi \int_0^r \mathrm{d}r' r'^2 \epsilon(r')$ is the gravitational mass inside a sphere of radius r. Therefore, if one can accurately measure two independent global parameters, such as gravitational mass (hereafter, mass M) and radius (R) of a non-spinning star, most of the theoretically proposed EoS models can be effectively ruled out. For a fast-spinning star, one needs to measure an additional parameter, e.g., the stellar spin frequency (ν). However, three required parameters have so far not been precisely measured for any neutron star.

Note that the recent precise measurement of the mass ($2.01 \pm 0.04 M_\odot$) of the millisecond pulsar PSR J0348+0432 rules out the EoS models which cannot support such a high mass value (Antoniadis *et al.* 2013). But, while this has somewhat constrained the parameter space, all types of EoS models, such as nucleonic, strange quark matter, hybrid and hyperonic still survive (Bhattacharyya *et al.* 2016, 2017).

Accurate measurements of three independent global parameters of the same neutron star is extremely

difficult because of a number of unknown systematics. However, such systematic uncertainties can be reduced if complementary methods to measure the stellar parameters are available for a given neutron star. A Low-Mass X-ray Binary (LMXB), in which a neutron star accretes matter from a Roche-lobe filling low-mass companion (Bhattacharyya 2009), can provide several such complementary methods, and hence can be a particularly promising system for parameter measurements (see, Bhattacharyya 2010 for a review). These methods involve various spectral and timing features, such as thermonuclear X-ray bursts and their various properties, accretion-powered pulsations, kilo-Hertz Quasi-Periodic Oscillations (kHz QPOs), broad relativistic iron lines, quiescent emissions and timing features due to orbital motion, as complementary tools to reliably measure neutron star parameters (Bhattacharyya 2010). Here, we focus on one of these methods, the one involving the broad relativistic iron line.

A broad relativistic iron Kα spectral emission line is observed from many stellar-mass and supermassive black hole systems (Fabian *et al.* 2000; Miller 2007; Reynolds & Nowak 2003). Such a fluorescent line near 6 keV is believed to originate from the reflection of hard X-rays from the geometrically thin accretion disc. The hard X-ray source could be an accretion disc corona (Fabian *et al.* 2000), or even the base of a jet (Markoff & Nowak 2004). An incident X-ray photon can either be Compton scattered by free or bound electrons, or be subject to photoelectric absorption. Such an absorption is followed by either Auger de-excitation or fluorescent line emission (Fabian *et al.* 2000). While many such lines are generated, the strongest among them is the one for the $n = 2 \rightarrow n = 1$ transition of the iron atom or ion. Such an intrinsically narrow iron line in the range 6.4–6.97 keV is broadened and shaped by various physical effects, e.g., Doppler effect, special relativistic beaming, gravitational redshift and general relativistic light-bending (Tanaka *et al.* 1995). Fitting the shape and energies of this line with an appropriate relativistic model can, therefore, be used to measure the inner-edge radius r_{in} of the accretion disc in the unit of the black hole mass M. By assuming that the disc extends up to the Innermost Stable Circular Orbit (ISCO), i.e., r_{in} is the ISCO radius r_{ISCO}, one can infer the black hole angular momentum parameter a from the known expression of $r_{ISCO}c^2/GM$ for the Kerr spacetime (Miller 2007). Here, $a = Jc/GM^2$, with J be the black hole angular momentum.

Note that r_{in} can evolve with accretion rate for a source, as the disc can be truncated at various
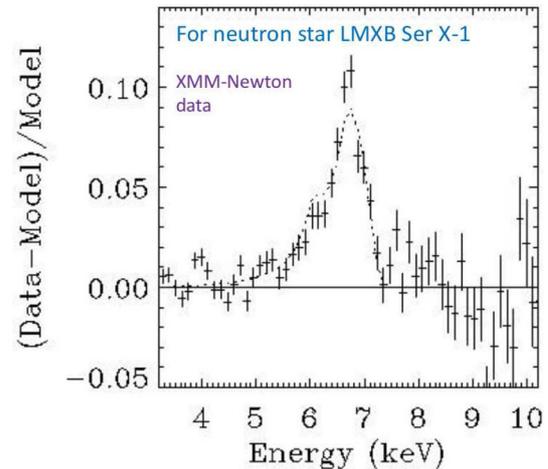

Figure 1. Relativistic iron Kα spectral emission line from the inner accretion disc of the neutron star LMXB Ser X–1 (*XMM-Newton* satellite data; Bhattacharyya & Strohmayer 2007). This line is shown as the X-ray intensity in excess to the best-fit continuum spectral model and normalized by this continuum model. A broad asymmetric line is clearly shown by the data points, which is well-fit with the dotted profile of a relativistic model (see section 1).

radii due to magnetic field, radiative pressure or other reasons. Therefore, the ISCO radius r_{ISCO} is the lower limit of r_{in} for an accreting black hole. Hence, the minimum inferred value of $r_{in}c^2/GM$ for a given black hole source can be considered an upper limit of $r_{ISCO}c^2/GM$, which gives the lower limit of the angular momentum parameter a of that source.

If the relativistic disc line were also observed from an accreting neutron star, then that could be used as a tool to measure stellar parameters, and hence to constrain EoS models. But, while a broad iron line from neutron star LMXBs had been known (see, for example, Asai *et al.* 2000), their characteristic asymmetry, and hence the relativistic nature and the inner disc origin, could not be established till 2006. In 2007, Bhattacharyya & Strohmayer (2007) established the inner accretion disc origin of the broad iron line from a neutron star LMXB for the first time (see Fig. 1). This was done by analysing the *XMM-Newton* satellite data from Serpens X–1 (Ser X–1), which opened a new area of science and supported the continuation of this satellite (McBreen & Schartel 2008).

In section 2, we outline the rapid development of the field of relativistic lines from neutron star LMXBs during the past decade. In section 3, we briefly describe how such a spectral line can be used to constrain stellar EoS models. Finally, we briefly mention our conclusions in section 4.
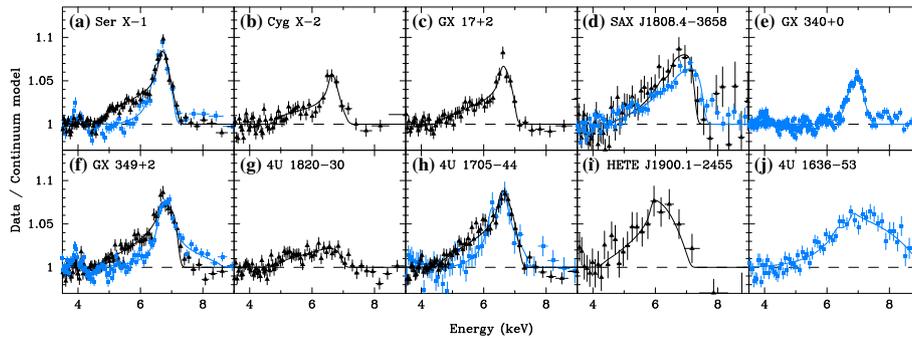
Figure 2. Examples of broad relativistic iron Kα spectral emission line from a number of neutron star LMXBs. Here, data to the continuum model ratio is shown. Best-fit relativistic models are shown by solid lines. *Suzaku* satellite data are displayed in black and the *XMM-Newton* satellite data are shown in blue (section 2; figure courtesy: Cackett *et al.* 2010).

2. Relativistic iron spectral line from neutron star LMXBs

Soon after the first detection of broad relativistic iron spectral emission line from the *XMM-Newton* data of Ser X–1 (Bhattacharyya & Strohmayer 2007), this line was confirmed from the same source with another satellite *Suzaku* (Cackett *et al.* 2008). This paper also reported such lines from the *Suzaku* data of two other neutron star LMXBs: 4U 1820–30 and GX 349+2, and found that the measured inner disc radii from iron lines of these two sources are consistent with the inner disc radii implied by the high-frequency timing feature kHz QPOs. Next, Pandel *et al.* (2008) reported the detection of a broad relativistic iron line from the *XMM-Newton* and *RXTE* satellite data of 4U 1636–536. This line feature indicated a combination of several iron Kα lines in different ionization states. Papitto *et al.* (2009) reported a highly significant iron Kα emission line from the *XMM-Newton* data of the accretion-powered millisecond pulsar SAX J1808.4–3658. Assuming a stellar mass of $1.4 M_{\odot}$, the inferred value of r_{in} was $18.0^{+7.6}_{-5.6}$ km. This was less than the pulsar corotation radius (31 km), which was consistent with the fact that the accretion-powered pulsations were observed during the iron line detection. Di Salvo *et al.* (2009) found not only a broad relativistic iron emission line from the *XMM-Newton* data of the neutron star LMXB 4U 1705–44, but also other broad low-energy emission lines from this source. These low-energy lines and the iron line appeared to be produced from the same inner disc region.

The new field of broad relativistic iron spectral emission line from neutron star systems evolved rapidly, and such a line was detected from 10 sources within just three years of the first detection (Cackett *et al.* 2010 and references therein). This paper presented a comprehensive, systematic analysis of *Suzaku* and *XMM-Newton* spectra of these sources, of which four are very bright and persistent Z sources, four are medium bright atoll sources, and two are accretion-powered millisecond pulsars (see Fig. 2). Cackett *et al.* (2010) suggested that the boundary layer of the neutron star illuminates the disc. Note that, a boundary layer does not exist in case of an accreting black hole, and a corona or the base of a jet provides the illuminating hard X-rays for black hole sources. Cackett *et al.* (2010) reported that $r_{in}c^2/GM =$ 6–15 for most cases. Moreover, although $r_{in}c^2/GM < 6$ values were not explored because Schwarzschild space-time was used, the best-fit $r_{in}c^2/GM$ value pegged at the lower limit 6 for many spectra. This implies that $r_{in}c^2/GM$ value could be somewhat smaller than 6 for many cases. However, unlike black hole systems, $r_{in}c^2/GM$ cannot be much smaller than 6, because the disc has to terminate at the hard surface of the neutron star.

Since the shapes of broad relativistic iron lines were measured with X-ray Charge-Coupled Devices (CCDs), pile-up could affect such measurements. In case of pile-up, two or more photons are registered as a single event during a given CCD frame, and thus pile-up can distort the spectrum. Therefore, for a bright source like a neutron star LMXB, the inferred relativistic nature of the iron emission line could be a result of pile-up. Hence, Miller *et al.* (2010) assessed the impact of this effect on relativistic disc lines, and found that a severe pile-up falsely narrows the emission lines. Therefore, the observed large width of such a line cannot be a result of the pile-up. Moreover, when the pile-up effect is modest, the relativistic disc spectroscopy is not significantly affected (see, for example, Fig. 11 of Miller *et al.* 2010).

When the *NuSTAR* satellite was launched, Ser X–1 was again observed with this satellite for two reasons: (1) the broadband capability (in 3–79 keV) of *NuSTAR* could characterize the source continuum spectrum in an
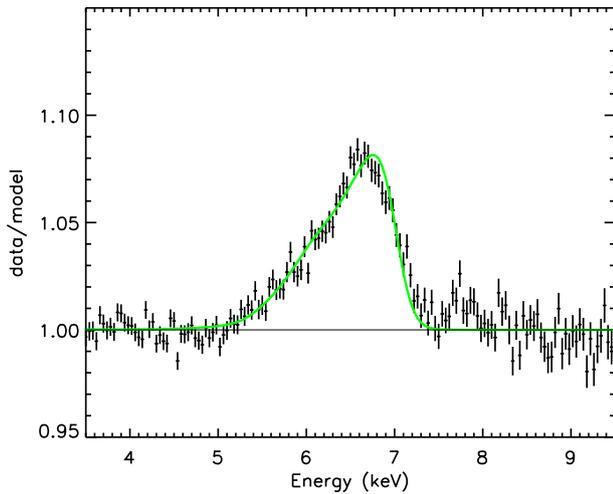
Figure 3. Broad relativistic iron Kα spectral line from the *NuSTAR* data of the neutron star LMXB Ser X–1. Data to continuum model ratio is shown. The green line shows the best-fit relativistic model (section 2; figure courtesy: Miller *et al.* 2013).

unprecedented manner, and (2) the ability of *NuSTAR* to measure the iron Kα line free of photon pile-up distortions (Miller *et al.* 2013). The relativistic nature of the broad iron Kα line detected with *NuSTAR*, which suggested a disc inner edge close to the ISCO, was 5σ significant (see Fig. 3). Moreover, a broad hump around $10-20$ keV in the continuum spectrum was detected for the first time from a neutron star LMXB. Such hump is expected from Compton back-scattering, and was earlier detected from a number of black hole systems. As if the confirmation of the relativistic disc line from three satellites were not enough, Ser X–1 was observed once again with the *Chandra* satellite (Chiang *et al.* 2016a). This longest (300 ks) observation with the 'High Energy

Transmission Grating Spectrometer' in the 'continuous clocking' mode was free of the pile-up effects and would detect narrow lines in the iron K range, if present. As expected, the relativistic nature of the line was clearly found (see Fig. 4). However, there was no strong evidence of narrow lines.

If the broad iron line is produced by the reflection of hard X-ray photons from the disc, then this line is expected to be delayed with respect to the illuminating hard X-ray source by the light travel time between this illuminating source and the disc. This delay could be manifested in the time-lag spectrum of kHz QPOs, which are believed to be produced close to the accreting neutron star. Indeed, Barret (2013) reported a clear lag of 3–8 keV photons with respect to 8–30 keV photons for a range of kHz QPO frequencies. The amount of this lag (∼15–40 μs) is consistent with the light travel time for a distance of a few Schwarzschild radii, that is a rough distance between the neutron star and the inner disc. Moreover, a tentative hump in the time-lag spectrum around the broad iron Kα line energy indicates that this line is a part of the delayed reflected spectrum (see Fig. 5). This, the observations of relativistic disc line from the same source with several satellites, and further detections and measurements of such lines from neutron star LMXBs with *NuSTAR* and other satellites (e.g., Chiang *et al.* 2016b; Ludlam *et al.* 2017a, b; Mondal *et al.* 2017) have firmly established this new field within a decade from the first detection.

3. Ways to constrain EoS models

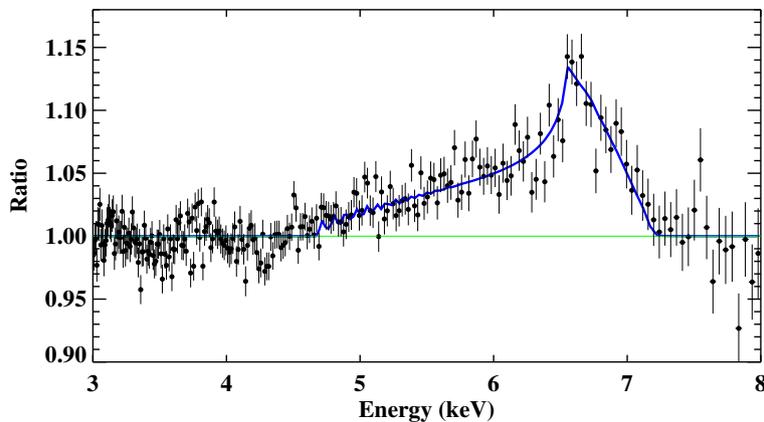In this section, we discuss how the dimensionless inner edge radius $r_{in}c^2/GM$ of the geometrically thin,

Figure 4. Broad relativistic iron Kα spectral line from the *Chandra* data of the neutron star LMXB Ser X–1. Data to continuum model ratio is shown. The blue line shows the best-fit relativistic model (section 2; figure courtesy: Chiang *et al.* 2016a).
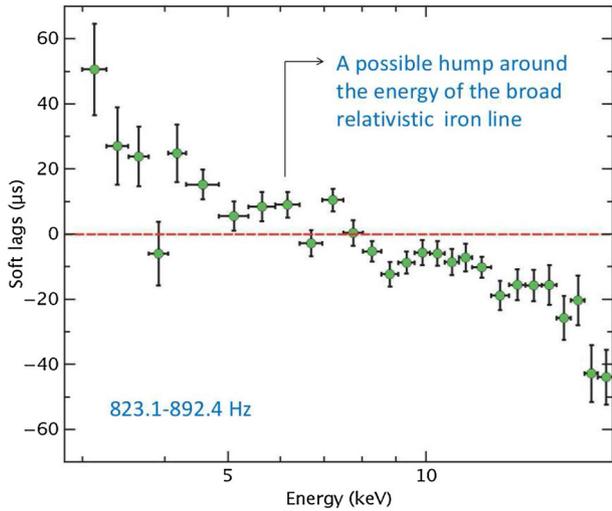
Figure 5. Mean time-lag energy spectrum for the kHz QPO frequency range (823.1–892.4 Hz) from the *RXTE* satellite data of the neutron star LMXB 4U 1608–522 (Barret 2013). A tentative hump around 5–7 keV is suggestive of the reflection origin of the iron line (section 2; figure courtesy: Barret 2013).

Keplerian disc, inferred from fitting the shape of a relativistic disc line, can be used to constrain neutron star EoS models. As mentioned in section 1, measurements of three independent stellar parameters are required to probe the EoS models. Here, we propose to use $r_{in}c^2/GM$ as one of these three parameters. More specifically, our method involves constraining the M versus $r_{in}c^2/GM$ space and/or the Rc^2/GM versus $r_{in}c^2/GM$ space in order to constrain EoS models. This

is because M and Rc^2/GM could be independently inferred for some neutron star LMXBs. For example, M could be measured by the binary orbital motion method (e.g., Steeghs & Casares 2002; Bhattacharyya 2010), while Rc^2/GM could be inferred using thermonuclear burst oscillations (e.g., Bhattacharyya *et al.* 2005). However, in order to rule out EoS models from the observational constraints on the above mentioned parameter spaces, one needs to theoretically compute $r_{in}c^2/GM$ for various EoS models.

Computation of $r_{in}c^2/GM$ for a neutron star is much more challenging than that for a black hole, because neutron star has a hard surface. For the time being, let us assume that the disc is not truncated at a higher radius by magnetic field, radiative pressure or other means (section 1). In such a case, $r_{in}c^2/GM$ can always be obtained from a known analytical expression of r_{ISCO} for a black hole (see section 1). But for a neutron star LMXB, the disc terminates either at the stellar radius R or at r_{ISCO}, whichever is bigger. Both R and r_{ISCO} depend on the stellar EoS, mass and the spin rate. Therefore, while $r_{in}c^2/GM$ of a corotating disc always decreases with an increasing a for a black hole, it can either decrease or increase with an increasing spin rate for a neutron star (see Fig. 6). In addition, $r_{in}c^2/GM$ depends on stellar mass and EoS. Hence, the computation of $r_{in}c^2/GM$ for a neutron star requires the calculation of the rapidly spinning stellar structure considering the full effect of general relativity. This is because the neutron stars in LMXBs are expected to be
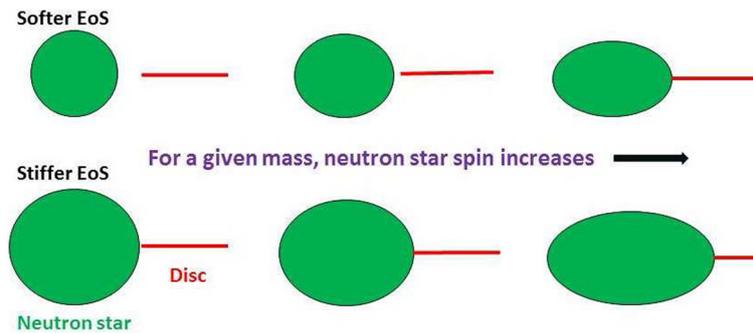

Figure 6. A cartoon showing the effects of neutron star EoS and spin rate on the location of the accretion disc inner edge. Here we assume that the disc terminates at the stellar surface or at the ISCO, whichever is bigger. For the same mass and spin rate, the neutron star is smaller for a softer EoS. In case of such an EoS and a smaller spin rate, it is more likely that the disc would not touch the stellar surface and would terminate at the ISCO. For a higher spin rate and the same mass and EoS, the stellar equatorial radius would increase and the (corotating) disc inner edge radius would likely decrease. But when the stellar equatorial radius becomes large enough for an even higher spin rate, the disc would terminate at the stellar surface instead of the ISCO radius, and the disc inner edge radius would naturally increase for a further increase of the spin rate. For a stiffer EoS model, the qualitative behaviour of the disc inner edge radius is the same, but, as the neutron star is bigger for this case, the disc could touch the star for a smaller spin rate. Note that the stellar deformation due to spin is exaggerated in this figure (see section 3).
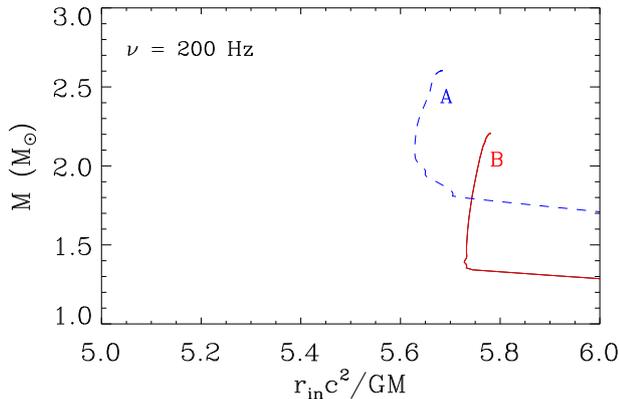
Figure 7. Neutron star mass versus disc inner edge radius-to-stellar-mass ratio for two realistic EoS models (*A* and *B*; see section 3) for a stellar spin frequency of 200 Hz (Bhattacharyya 2011). The straight line portions of the curves correspond to the disc termination on the stellar surface. This figure shows how a measurement of the disc inner edge radius-to-stellar mass ratio from the fitting of a broad relativistic iron Kα spectral line can be used to constrain neutron star EoS models, when the stellar spin frequency is known.

rapidly spinning (spin frequency $\nu \sim$ a few hundred Hz), and hence a non-spinning approximation for stellar structure calculation will not serve our purpose, as we are looking for the effects of the stellar spin rate on $r_{in}c^2/GM$.

The method to numerically compute a rapidly spinning neutron star structure, and thus to calculate R, r_{in} and other stellar parameters for a given EoS model, were detailed in a number of papers (Bhattacharyya *et al.* 2000, 2001a, b, c; Bhattacharyya 2002; Cook *et al.* 1994; Datta *et al.* 1998), and we will not repeat it here. In fact, Bhattacharyya (2011) calculated r_{in} for $\sim$16000 stable neutron star structures. Here, we review the method mentioned in Bhattacharyya (2011), as currently this is the only paper that reported a detailed procedure to constrain EoS models using relativistic disc lines. Here, for the purpose of demonstration, we use two theoretically proposed nucleonic EoS models, which can support the maximum observed neutron star mass ($2.01 \pm 0.04 M_\odot$; section 1). These EoS models are briefly described here. (1) *Model A*: this is the stiffer EoS model among the two, and is a field theoretical chiral sigma model for neutron-rich matter in beta equilibrium (Sahu *et al.* 1993). (2) *Model B*: this is the argonne v_{18} model of two-nucleon interaction, including the three-nucleon interaction (Urbana IX [UIX] model) and also the effect of relativistic boost corrections (Akmal *et al.* 1998).

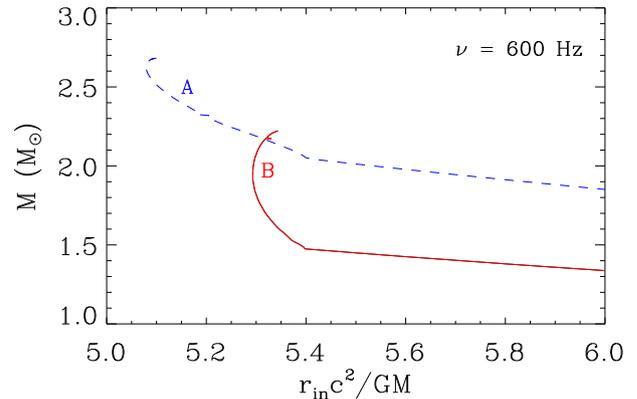We demonstrate the ways to constrain EoS models for an inferred $r_{in}c^2/GM$ value using Figures 7–10.

Figure 8. Similar to Fig. 7, but for a stellar spin frequency of 600 Hz (Bhattacharyya 2011; see also section 3).
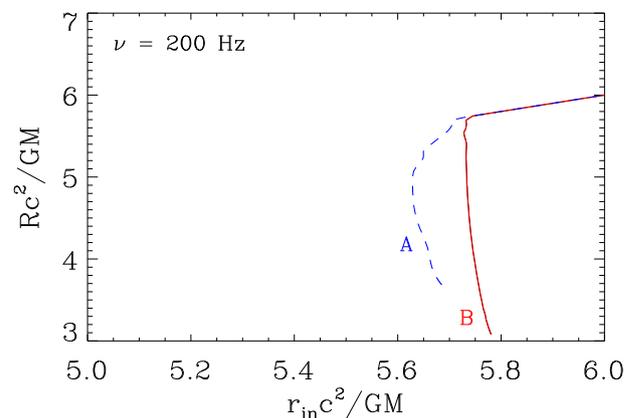

Figure 9. Neutron star radius-to-mass ratio versus disc inner edge radius-to-stellar mass ratio for two realistic EoS models (A and B; see section 3) for a stellar spin frequency of 200 Hz (Bhattacharyya 2011). The straight line portions of the curves correspond to the disc termination on the stellar surface. This figure shows how a measurement of the disc inner edge radius-to-stellar-mass ratio from the fitting of a broad relativistic iron Kα spectral line can be used to constrain neutron star EoS models, when the stellar spin frequency is known.

We assume a known value of ν for each case, because ν is measured for a number of neutron star LMXBs (Patruno & Watts 2012; Watts 2012). Note that we consider $r_{in}c^2/GM$ up to 6 in these figures. This is because $r_{ISCO}c^2/GM = 6$ for a non-spinning neutron star and $r_{ISCO}c^2/GM < 6$ for $\nu > 0$ for a corotating disc. Therefore, when $r_{in}c^2/GM < 6$, the stellar spin certainly affects $r_{in}c^2/GM$, which is required to distinguish various EoS model curves using the inferred $r_{in}c^2/GM$ value (Figures 7–10). Note that observations indicate $r_{in}c^2/GM < 6$ for many cases, as mentioned in section 2.

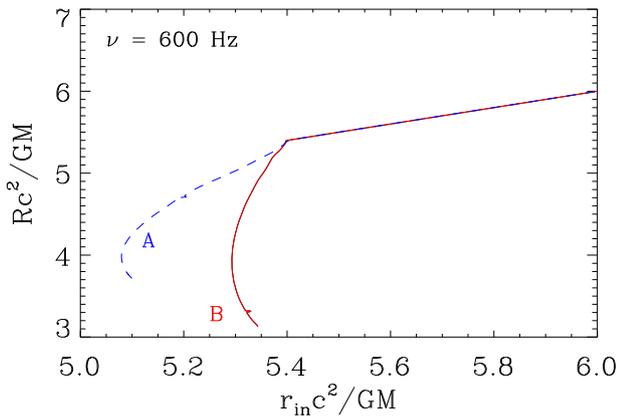The oblique straight line portions of the curves in Figures 7–10 are for $r_{in} = R$, while the other portions

Figure 10. Similar to Fig. 9, but for a stellar spin frequency of 600 Hz (Bhattacharyya 2011; see also section 3).

are for $r_{\rm in} = r_{\rm ISCO}$. These figures show that observed constraints on M (and/or Rc^2/GM) and $r_{\rm in}c^2/GM$ can constrain EoS models. However, one needs to measure $r_{\rm in}c^2/GM$ typically with better than 0.1 accuracy in order to distinguish curves for various EoS models.

While constrining EoS models, if we assume that the inferred $r_{\rm in}c^2/GM$ is exactly same as the numerically computed $r_{\rm in}c^2/GM$ (i.e., Rc^2/GM or $r_{\rm ISCO}c^2/GM$, whichever is greater), then systematics will be introduced in such constraints. This is because, even when the inferred $r_{\rm in}c^2/GM$ is less than 6, the disc inner edge radius can be affected by stellar magnetic field, radiative pressure or other effects, and the disc could be truncated at a slightly higher radius value than R and $r_{\rm ISCO}$. Therefore, the observationally inferred $r_{\rm in}c^2/GM$ should be taken as the upper limit, while comparing with the numerical results shown in Figures 7–10. Note that EoS models can be effectively constrained even with this upper limit. For example, a suitable value of the measured upper limit of $r_{\rm in}c^2/GM$ can rule out softer EoS models, even if neither M nor Rc^2/GM is measured (Figures 7–10). Moreover, if an upper limit of M is known in addition to the upper limit of $r_{\rm in}c^2/GM$, then some of the stiffer EoS models could be ruled out (see Figures 7–8).

4. Conclusion

Relativistic disc line from neutron star systems is a decade-old field. While this new field is already well established by many detections of such a line, its utility to constrain neutron star EoS models is not yet well explored. Here we review the rapid development of this field and its current status. We also discuss how a relativistic disc line, which provides the accretion disc inner edge radius to stellar mass ratio, can be used to effectively constrain neutron star EoS models, if this ratio is measured with an accuracy better than 0.1. This accuracy could be achieved for a reasonable exposure with a future X-ray satellite, such as *eXTP* and *Athena*.

References

Akmal, A., Pandharipande, V. R., Ravenhall, D. G. 1998, *Phys. Rev. C*, **58**, 1804.

Antoniadis J., Freire P. C. C., Wex N. *et al.* 2013, *Science*, **340**, 448.

Asai, K., Dotani, T., Nagase, F., Mitsuda, K. 2000, *ApJS*, **131**, 571.

Barret, D. 2013, *ApJ*, **770**, 9.

Bhattacharyya, S. 2002, *A&A*, **383**, 524.

Bhattacharyya, S. 2009, *Current Science*, **97**, 804.

Bhattacharyya, S. 2010, *Advances in Space Research*, **45**, 949.

Bhattacharyya, S. 2011, *MNRAS*, **415**, 3247.

Bhattacharyya, S., Bombaci, I., Bandyopadhyay, D., Thampan, A. V., Logoteta, D. 2017, *New Astronomy*, **54**, 61.

Bhattacharyya, S., Bombaci, I., Logoteta, D., Thampan, A. V. 2016, *MNRAS*, **457**, 3101.

Bhattacharyya, S., Strohmayer, T. E. 2007, *ApJ*, **664**, L103.

Bhattacharyya, S., Strohmayer, T. E., Miller, M. C., Markwardt, C. B. 2005, *ApJ*, **619**, 483.

Bhattacharyya S., Thampan A. V., Misra R., Datta B. 2000, *ApJ*, **542**, 473.

Bhattacharyya S., Bhattacharya D., Thampan A. V. 2001a, *MNRAS*, **325**, 989.

Bhattacharyya S., Misra R., Thampan A. V. 2001b, *ApJ*, **550**, 841.

Bhattacharyya S., Thampan A. V., Bombaci I. 2001c, *A&A*, **372**, 925.

Blaschke, D., Klaehn, T., Weber, F. 2008, *Contribution to Proceedings of the 3rd International Workshop on Astronomy and Relativistic Astrophysics (IWARA)*.

Cackett, E. M., Miller, J. M., Ballantyne, D. R. *et al.* 2010, *ApJ*, **720**, 205.

Cackett, E. M., Miller, J. M., Bhattacharyya, S. *et al.* 2008, *ApJ*, **674**, 415.

Chiang, C.-Y., Miller, J. M., Cackett, E. M. *et al.* 2016a, *ApJ*, **821**, 105.

Chiang, C.-Y., Morgan, R. A., Cackett, E. M., Miller, J. M., Bhattacharyya, S., Strohmayer, T. E. 2016b, *ApJ*, **831**, 45.

Cook G. B., Shapiro S. L., Teukolsky S. A. 1994, *ApJ*, **424**, 823.

Datta B., Thampan A. V., Bombaci I. 1998, *A&A*, **334**, 943.

di Salvo, T., D'Aí, A., Iaria, R. 2009, *MNRAS*, **398**, 2022.

Fabian, A. C., Iwasawa, K., Reynolds, C. S., Young, A. J. 2000, *PASP*, **112**, 1145.

Lattimer, J. M., Prakash, M. 2007, *Physics Reports*, **442**, 109.

Ludlam, R. M., Miller, J. M., Bachetti, M. *et al.* 2017a, *ApJ*, **836**, 140

Ludlam, R. M., Miller, J. M., Cackett, E. M., Degenaar, N., Bostrom, A. C. 2017b, *ApJ*, **838**, 79

Markoff, S., Nowak, M. A. 2004, *ApJ*, **609**, 972.

McBreen, B., Schartel, N. 2008, *Astron. Nachr.*, **329**, 226.

Miller, J. M. 2007, *ARA&A*, **45**, 441.

Miller, J. M., D'Aí, A., Bautz, M. W. 2010, *ApJ*, **724**, 1441.

Miller, J. M., Parker, M. L., Fuerst, F. *et al.* 2013, *ApJ*, **779**, L2.

Mondal, A. S., Pahari, M., Dewangan, G. C., Misra, R., Raychaudhuri, B. 2017, *MNRAS*, **466**, 4991

Özel, F., Psaltis, D. 2009, *PRD*, **80**, 103003.

Pandel, D., Kaaret, P., Corbel, S. 2008, *ApJ*, **688**, 1288.

Papitto, A., Di Salvo, T., D'Aí, A., Iaria, R., Burderi, L., Riggio, A., Menna, M. T., Robba, N. R. 2009, *A&A*, **493**, L39.

Patruno, A., Watts, A. L. 2012, in: *Timing neutron stars: pulsations, oscillations and explosions*, edited by T. Belloni, M. Mendez & C. M. Zhang, ASSL, Springer (arXiv:1206.2727).

Reynolds, C. S., Nowak, M. A. 2003, *Physics Reports*, **377**, 389.

Sahu, P. K., Basu, R., Datta, B. 1993, *ApJ*, **416**, 267.

Steeghs, D., Casares, J. 2002, *ApJ*, **568**, 273.

Tanaka, Y., Nandra, K., Fabian, A. C. *et al.* 1995, *Nature*, **375**, 659.

van Kerkwijk, M. H. 2004, in: *Compact Stars: The Quest for New States of Dense Matter*, edited by D. K. Hong, C.-H. Lee, H. K. Lee, D.-P. Min, T.-S. Park & M. Rho, World Scientific Publishing Company: Singapore, 116.

Watts, A. L. 2012, *ARA&A*, **50**, 609.